Magnetic reconnection and cold plasma at the magnetopause

M. André,[1] A. Vaivads,[1] Y. V. Khotyaintsev,[1] T. Laitinen,[1] H. Nilsson,[2] G. Stenberg,[2] A. Fazakerley,[3] and J. G. Trotignon[4]

Received 7 July 2010; revised 3 August 2010; accepted 10 August 2010; published 25 November 2010.

[1] We report on detailed observations by the four Cluster spacecraft of magnetic reconnection and a Flux Transfer Event (FTE) at the magnetopause. We detect cold (eV) plasma at the magnetopause with two independent methods. We show that the cold ions can be essential for the electric field normal to the current sheet in the separatrix region at the edge of the FTE and for the associated acceleration of ions from the magnetosphere into the reconnection jet. The cold ions have small enough gyroradii to drift inside the limited separatrix region and the normal electric field can be balanced by this drift, $\mathbf{E} \approx -\mathbf{v} \times \mathbf{B}$. The separatrix region also includes cold accelerated electrons, as part of the reconnection current circuit. **Citation:** André, M., A. Vaivads, Y. V. Khotyaintsev, T. Laitinen, H. Nilsson, G. Stenberg, A. Fazakerley, and J. G. Trotignon (2010), Magnetic reconnection and cold plasma at the magnetopause, *Geophys. Res. Lett.*, *37*, L22108, doi:10.1029/2010GL044611.

1. Introduction

[2] Magnetic reconnection is a major mechanism in space and astrophysical plasmas for converting energy stored in magnetic fields into particle kinetic energy and for exchange of mass, energy and momentum between differently magnetized plasma regions. In near-earth space many properties of reconnection can be studied by spacecraft [*Paschmann*, 2008]. We use observations at the magnetopause by the Cluster spacecraft with multi-scale separation. The point of this investigation is to study both the properties of the magnetopause, including plasma composition, and the fundamentals of reconnection, including the origin of the electric fields accelerating particles.

[3] Flux transfer events, FTEs, are often-observed manifestations of time-varying reconnection at the magnetopause [*Khotyaintsev et al.*, 2004; *Owen et al.*, 2008; *McFadden et al.*, 2008; *Fear et al.*, 2008]. We investigate an event where the spacecraft are located just inside the magnetopause, and during an FTE are hit by a bulge including a jet of particles from a reconnection X-line near the subsolar point. We show that the plasma just inside the magnetopause is dominated by cold (eV) ions [*Sauvaud et al.*, 2001; *Chandler and Moore*, 2003; *McFadden et al.*, 2008]. We add to previous observations of cold plasma in this region by using a technique based on detection of a wake electric field caused by cold ions streaming past a charged spacecraft [*Engwall et al.*, 2009a]. Fundamental properties of reconnection can be studied by investigating the separatrix region between the separatrix, the magnetic field line connected to the reconnection X-line, and the ion jet ejected by the reconnection process. Several studies investigate the kinetic properties of the separatrix region at the magnetopause where the frozen-in condition is broken and ions can be accelerated into the reconnection jet by an electric field normal to the large-scale jet region [*Mozer et al.*, 2002; *Vaivads et al.*, 2004; *Khotyaintsev et al.*, 2006; *Retinò et al.*, 2006; *Lindstedt et al.*, 2009]. We show that the cold ions entering the separatrix region can be essential for the normal electric field and the associated potential drop between the magnetosphere and the reconnection jet. The origin of the cold plasma can be plumes detached from the plasmasphere [*Goldstein et al.*, 2004; *McFadden et al.*, 2008]. Consistent with this scenario, we observe cold accelerated electrons as part of the reconnection current circuit.

2. Observations and Interpretation

[4] During the spring of 2008, the four Cluster spacecraft several times crossed the subsolar magnetopause with a multi-scale satellite separation. On March 3, around 23:15 UT, the distance between Cluster 3 and 4 (C3, C4) was ~35 km, with distances to C1 and C2 of ~8000 km (Figures 1a and 1b). For comparison, the ion inertial lengths are about 130 and 360 km (magnetosheath and magnetosphere) and the corresponding electron gyroradii are about 3 and 10 km. The spacecraft are essentially in the plane of the magnetopause, moving much slower than the plasma phenomena we investigate. The direction of the interplanetary magnetic field (IMF) observed by the ACE spacecraft is consistent with Cluster observations in the magnetosheath and is indicated in Figure 1b. We use Cluster data from the EFW wire boom electric field instrument, the FGM fluxgate magnetometer, the CIS/HIA ion spectrometer, the PEACE electron instrument and the WHISPER sounder [*Escoubet et al.*, 2001, and references therein].

[5] Figures 1c–1e give an overview of the magnetopause crossing we study. Figure 1c shows the magnetic field from C3. The satellite is first located in the magnetosphere, as indicated by the dominating B_Z (GSM) component up to around 23:16 UT, and is later in the magnetosheath, as indicated by the varying but mainly south-west magnetic field. The ion velocity in Figure 1d shows that C3 is hit by jets along the magnetopause plane 23:06–23:11, 23:12–23:13 and 23:16–23:20 UT (the nearby C4 is hit by the same jets, not shown). The jets before 23:11 UT are interpreted as multiple FTEs moving in different directions, probably due to a moving reconnection X-line or multiple X-lines, indicating that the X-lines are not too far away (within a few Earth radii, R_E) [*Laitinen et al.*, 2010]. We concentrate on the

[1] Swedish Institute of Space Physics, Uppsala, Sweden.
[2] Swedish Institute of Space Physics, Kiruna, Sweden.
[3] Mullard Space Science Laboratory, Dorking, UK.
[4] Laboratoire de Physique et Chimie de l'Environnement et de l'Espace, Université d'Orléans, Orléans, France.

0094-8276/10/2010GL044611

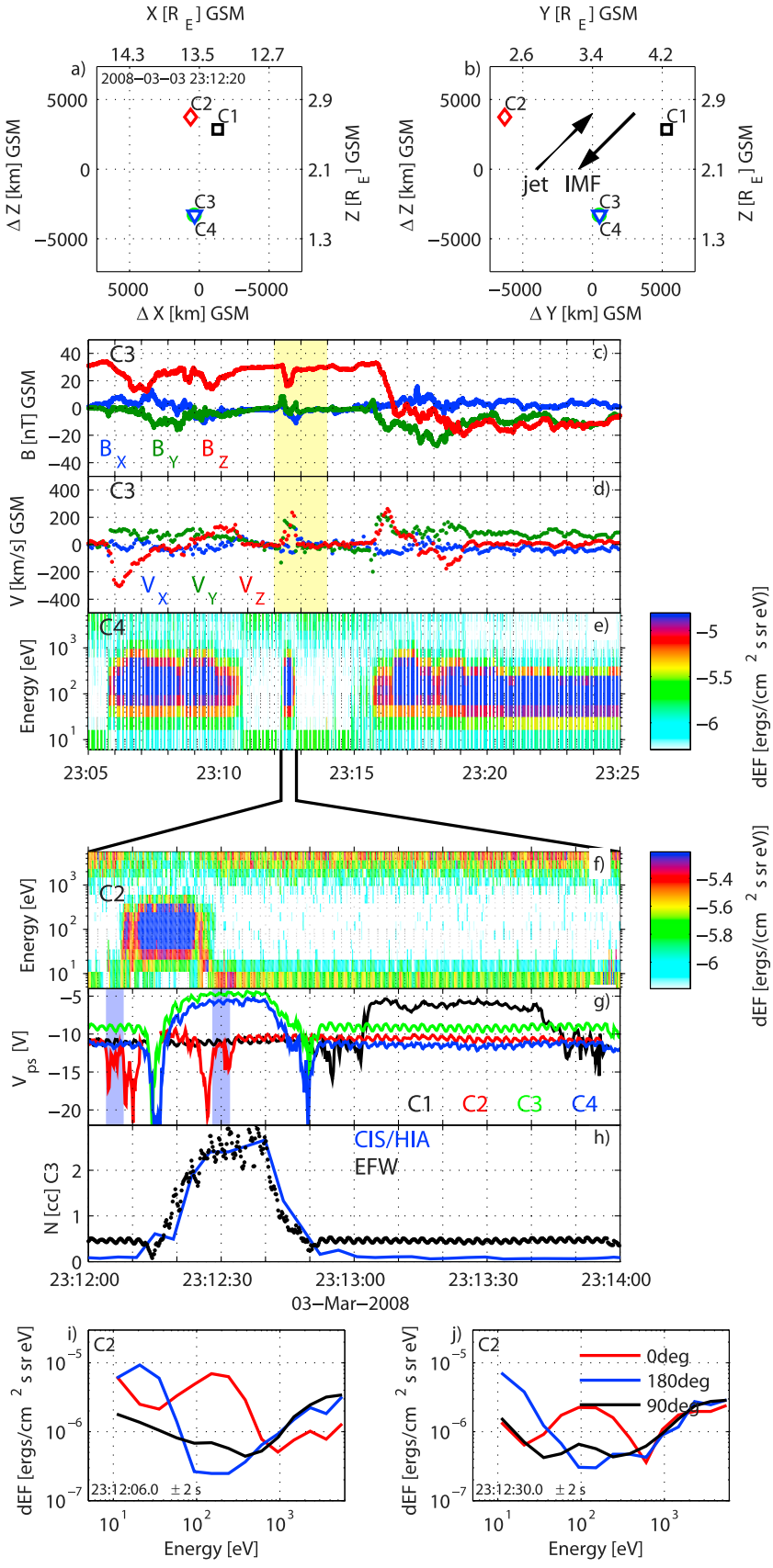
X [R E] GSM
Y [R E] GSM
a)
b)
2008–03–03 23:12:20
C1
C2
C3
C4
jet
IMF
Δ Z [km] GSM
Z [R E] GSM
Δ X [km] GSM
Δ Y [km] GSM
B [nT] GSM
V [km/s] GSM
Energy [eV]
dEF [ergs/(cm 2 s sr eV)]
c)
d)
e)
f)
g)
h)
i)
j)
V_{ps} [V]
N [cc] C3
CIS/HIA
EFW
03–Mar–2008
23:12:06.0 ± 2 s
23:12:30.0 ± 2 s
0deg
180deg
90deg

Figure 1

jet observed by C3 during 23:12–23:13 UT, indicated in yellow, with a direction as indicated in Figure 1b. This jet is interpreted as an FTE originating at an X-line around the subsolar point. This interpretation is consistent with the bi-polar (positive-negative) behavior of the normal magnetic component (essentially B_X) (Figure 1c). The interpretation is also consistent with C4 electron data (which has higher resolution than C3 electron data during his event) with magnetosheath-like, 100 eV electrons and disappearing magnetospheric keV plasma (Figure 1e). This jet is selected since it is an example of an isolated and clear FTE observed with Cluster multi-scale separation and with a mixture of cold and hot plasmas (few eV to hundreds of eV) as discussed later.

[6] Figures 1f–1h give details of the jet of interest. Figure 1g shows the negative of all four spacecraft potentials, V_{ps}, as an indication of the density [*Pedersen et al.*, 2008]. Comparing with Figure 1b, we find that the FTE jet touches C2 (a small density increase, i.e., a small increase of V_{ps} above −10 V) and passes C3/4 and then C1 (a higher density increase on all these spacecraft). All satellites show a decrease of V_{ps} at the edges of the jet, which we interpret as at least partly being due to a density decrease. Such a decrease (in the separatrix region) is consistent with earlier observations [*Khotyaintsev et al.*, 2006] and simulations [*Tanaka et al.*, 2008]. The decrease is deeper at C2/3/4, while it is less deep and more spread out at C1, i.e., further away from the X-line and later in the development of the FTE.

[7] Figure 1f shows an electron spectrogram from C2 (the spacecraft with the highest resolution electron data during this event). Note the hundred eV jet of magnetosheath electrons, and the disappearance of keV magnetospheric electrons at the same time, all consistent with a reconnection jet. Figure 1h shows densities from C3. The density from the CIS/HIA ion instrument can be compared with the total density from the spacecraft potential, outside the jet calibrated by the plasma frequency obtained from active sounding with the WHISPER instrument, and inside the jet by the CIS/HIA data (no clear Langmuir wave observations are available inside the FTE). Outside the FTE, densities measured by CIS/HIA are lower than estimates from the spacecraft potential. This is not surprising since cold (eV) ions can not reach a satellite charged to +10 V (Figure 1g), consistent with previous observations of cold plasma near the magnetopause [*Sauvaud et al.*, 2001].

[8] Figures 1i and 1j show C2 electron spectra from the edges of the FTE. Figures 1i and 1j are averaged over one satellite spin of 4 s. The time periods are chosen to cover the outer parts of the separatrix regions (indicated in Figure 1g). Figure 1i, from the first separatrix region, includes magnetospheric electrons with higher energies (>1 keV). At these energies, 0 degree pitch-angle away from the X-line, has lower fluxes. This is consistent with a loss of the magnetospheric source on newly reconnected magnetic field-lines [*Khotyaintsev et al.*, 2006]. At energies of a few 100 eV, accelerated magnetosheath electrons are moving away from the X-line at 0 degree pitch-angle, but not at other angles since this is the edge of the FTE. At energies below 50 eV electrons toward the X-line dominate, consistent with cold (eV) electrons originating in the ionosphere and being part of the reconnection Hall current circuit. Figure 1j gives similar results as Figure 1i, but with the decrease in flux away from the X-line above 1 keV being less clear and the increase toward the X-line at low energies being clearer. This can be due to sampling at slightly different times within Figures 1i and 1j. The difference between Figures 1i and 1j indicate the uncertainties in the spectra. We find the electron observations consistent with the edge of an FTE at intermediate and high energies, and also consistent with the presence of electrons of ionospheric origin participating in the reconnection current circuit in the separatrix region.

[9] Figure 2 gives more evidence of cold ions, and details concerning the separatrix region. Concentrating on the first edge of the jet, Figure 2a shows three components of the C4 magnetic field in an L, N, M-coordinate system obtained from minimum variance analysis of B, with N normal to the current sheet, L as close as possible to GSM Z-direction and M closing the system. Distances given at the top of Figure 2 are obtained from time differences of structures passing both C3 and C4 (arbitrary zero, distance along the N-direction, close to both the GSM x-direction and the vector from C4 to C3). Figure 2b gives currents estimated from C3 and C4, assuming current sheets are planar with the normal in the N direction and using the difference in magnetic field between the spacecraft to estimate the current density. Using single satellite observations and an estimate of the sheet velocity gives similar results. Figure 2c gives an estimate of the density from the spacecraft potential. Figure 2d shows the electric field E_N normal to the current sheet obtained in different ways. In order to investigate the separatrix region we use the generalized Ohm's law for the normal component neglecting electron inertial terms [*Khotyaintsev et al.*, 2006]

$$\mathbf{E} = -\mathbf{v} \times \mathbf{B} + \mathbf{j} \times \mathbf{B}/ne - \nabla p_e/ne$$

Before 23:12:13 UT the E field measured by the EFW wire boom instrument is modulated by the spacecraft spin, and is clearly different from $-\mathbf{v} \times \mathbf{B}$. The EFW double probe instrument measures the local electric field created when cold ions drifting with speeds higher than their thermal speed cause a wake behind the spacecraft. This wake is created when the spacecraft potential (here about +10 V (Figure 1g)) exceeds the equivalent drift energy of the ions (here up to

Figure 1. Magnetopause FTE. (a and b) Location of the Cluster spacecraft with a separation between C3 and C4 of 35 km and C3 at [13.5 3.5 1.6] R_E (GSM). The YZ-plane corresponds closely to the magnetopause plane. The reconnection jet (FTE) and IMF directions are indicated; (c) C3 magnetic field (GSM); (d) C3 ion drift velocities (GSM); (e) C4 electron spectrogram close to perpendicular direction; (f) C2 electron spectrogram close to perpendicular direction; (g) negative of the spacecraft potential for all satellites as an indication of the density; (h) density from C3 CIS/HIA ion observations, and density from EFW potential calibrated to observations of the plasma frequency from WHISPER active sounding outside high density FTE and to CIS/HIA inside the FTE; (i and j) electron spectra, corrected for spacecraft potential, from the separatrix regions at the edges of the FTE (indicated in Figure 1g). The FTE occurs in a plasma dominated by cold (<10 eV) ions, and cold accelerated (<50 eV) electrons are found in the separatrix regions at the edges of the FTE.

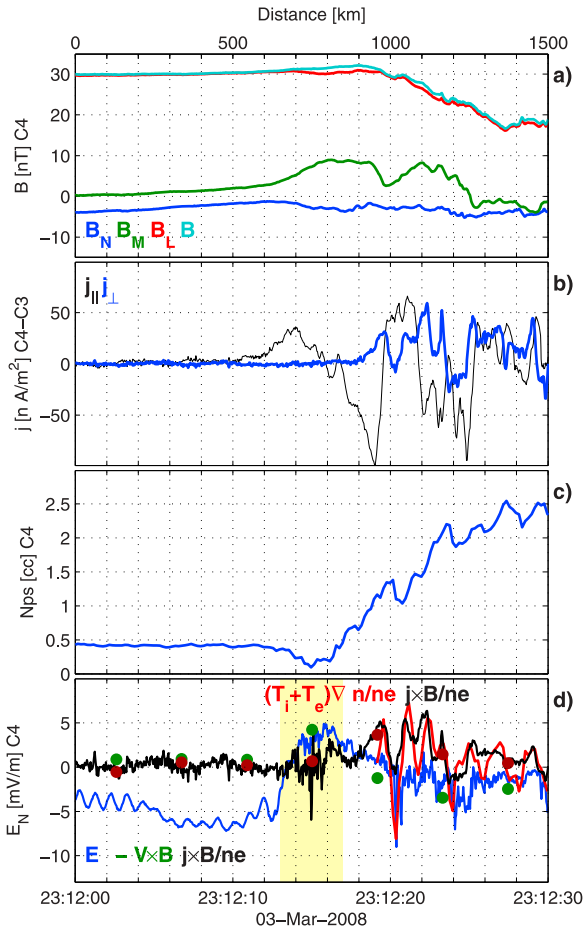

Figure 2. Separatrix region. (a) C4 magnetic field components in an L, N, M coordinate system with N being normal to the separatrix current sheet; (b) currents perpendicular and parallel to the magnetic field; (c) density; (d) E_N from the EFW wire boom instrument (blue line), $-(\mathbf{v} \times \mathbf{B})_N$ from FGM and CIS/HIA onboard particle moments (green dots), $(\mathbf{j} \times \mathbf{B}/ne)_N$ by combining Figures 2a–2c (black line), $\nabla(p_i + p_e)_N$ using constant particle temperatures and Figure 2c (red line) and $\nabla(p_i)_N$ from CIS/HIA onboard particle moments (red dots). N = [0.97 −0.23 −0.08], M = [0.23 0.97 0.00], L = [0.08 −0.02 0.99] GSM. E_N is balanced by $-(\mathbf{v} \times \mathbf{B})_N$ drifting ions in the separatrix region (indicated in yellow), and cold (eV) ions are present just outside this region.

10 eV). This shows that the plasma before 23:12:13 UT is dominated by cold ions, consistent with Figure 1h. Similar EFW observations have been used by *Engwall et al.* [2009b, 2009a] to estimate the outflow of cold ions in the magnetotail lobes. The $-\mathbf{v} \times \mathbf{B}$ estimate is computed from the CIS/HIA ion (mainly ~10 keV) drift ($\mathbf{v}$) observations (at spacecraft spin 4 s resolution) and the FGM magnetic field ($\mathbf{B}$) measurements. This estimate is not affected by the relatively small satellite potential, but can not be used to study the FTE edges/separatrices with high resolution.

[10] After 23:12:13 UT the EFW electric field suddenly changes direction, shows no signs of contamination from a local wake, and is a reliable observation of the local geophysical field. In part of the separatrix region, at least from 23:12:14 to 23:12:17 UT (indicated in yellow in Figure 2d), the electric field is strong and approximately equal to the ion $-\mathbf{v} \times \mathbf{B}$ term (from the onboard ion moment obtained during this spacecraft spin). Here ions with energies from tens to hundreds eV have gyroradii of ~20 to ~70 km, and can drift within a layer a few hundred km wide. The same event has been studied by *Vaivads et al.* [2010] where it has been suggested that the region of strong electric fields is an Alfvén edge from the reconnection site. We conclude that $-\mathbf{v} \times \mathbf{B}$-drifting rather cold plasma in the separatrix region can balance the normal electric field.

[11] In other observations of separatrix regions, E_N is often balanced by the $\mathbf{j} \times \mathbf{B}/ne$ term [*Vaivads et al.*, 2004; *Khotyaintsev et al.*, 2006]. After about 23:12:19 UT, $\mathbf{j} \times \mathbf{B}/ne$ is significant but does not correspond to E_N. To estimate plasma pressure gradients, we use a constant magnetosheath temperature of ~500 eV and ~100 eV for ions and electrons respectively (possible after 23:12:19 UT) and variations in the density (Figure 2c). Figure 2d shows that $\mathbf{j} \times \mathbf{B}/ne$ agrees well with the total pressure gradient. This is expected from the pressure balance equation in the case when off-diagonal terms in the pressure tensor, and plasma inertial effects, are negligible

$$\mathbf{j} \times \mathbf{B} = \nabla(p_i + p_e)$$

Plasma pressure gradients can also be estimated using CIS/HIA onboard ion moments, available at 4 s satellite spin resolution (Figure 2d, red dots). After 23:12:19 UT, these moments agree with the estimate using a constant plasma temperature, and density variations (Figure 2d, red line). At earlier times, the onboard ion moments give values close to zero. Gradients of the electron pressure are likely to give a smaller contribution since ion pressure is larger than electron pressure both in the magnetosphere and the magnetosheath. Thus, $\mathbf{j} \times \mathbf{B}/ne$ and pressure gradients are not important for the strong E_N observed by EFW in the separatrix region 23:12:14 to 23:12:17 UT.

[12] Considering the region where EFW reliably observes the geophysical electric field, we can estimate the potential difference across the C4 edge/separatrix region, 23:12:13–17 UT. Using the normal direction, and timing when magnetic field and density gradients pass over C3 and C4, gives a normal boundary velocity of about 50 km/s. The normal is mainly in the GSM x-direction, so taking 2–4 mV/m over 3–5 s (Figure 2d) gives a separatrix potential drop of 300–1000 V, slightly smaller than other events [*Lindstedt et al.*, 2009].

[13] Figure 3 shows FTE ion observations from C1, which has the highest ion data resolution during this event. The two columns include ion fluxes from two consecutive 4 s time periods. The upper panels show the ion jet with magnetosheath plasma together with cold plasma of magnetospheric origin, both $\mathbf{E} \times \mathbf{B}$ drifting eastward with about 200 km/s. The lower panels also show the cold plasma, during the same intervals. Our interpretation is that the FTE/reconnection jet consists of accelerated plasma from the magnetosheath, while the cold plasma with near zero parallel velocity has crossed the jet separatrix region locally.

3. Summary and Conclusions

[14] We confirm previous observations of cold (eV) ions inside the magnetopause. This is done by comparing total

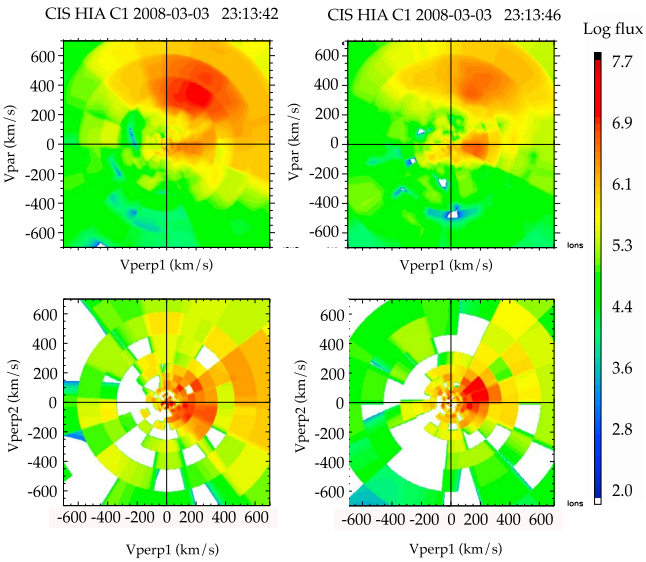

Figure 3. FTE ions. C1 ion fluxes (1/cm^2 s sr keV, assumed to be H^+) from two consecutive 4 s time periods, starting at 23:13:42 UT. (top) Ion distributions in the direction parallel to B versus one perpendicular direction, averaged over ±700 km/s in the second perpendicular direction; (bottom) fluxes averaged over ±100 km/s in the parallel direction, versus the two perpendicular directions. Cold accelerated ions originating inside the magnetosphere can be seen at approximately $v_{\|} = 0$, $v_{\perp} = 200$ km/s.

density (from spacecraft potential and the plasma frequency) with ion densities at energies above a few eV (from ion detectors on a positively charged spacecraft). These observations are consistent with results based on detection of a wake electric field caused by ions streaming past a charged spacecraft. This latter method gives high resolution and shows that cold plasma is present up to the reconnection separatrix. We find that the cold ions can be accelerated perpendicularly across a separatrix region at the magnetospheric edge of an FTE. At this edge also accelerated parallel cold electrons originating from the ionosphere are observed, as part of the reconnection current circuit. Inside the FTE the heated, but still rather cold, ions are observed together with ions of magnetosheath origin.

[15] A general plasma physics result is that cold ions affect the electric field in the separatrix region (and hence the potential drop across the region). The strong normal electric field can be balanced by $-\mathbf{v} \times \mathbf{B}$ drift of ions. In many events the ions are hot and have gyroradii larger than the narrow separatrix region [*Lindstedt et al.*, 2009]. In our case, the cold ions have small enough gyroradii to drift inside the limited separatrix region and can hence be important for the normal electric field.

[16] **Acknowledgments.** We thank the Cluster FGM team and Stephan Buchert for data analysis, and the ACE team for providing IMF data.

References

Chandler, M. O., and T. E. Moore (2003), Observations of the geopause at the equatorial magnetopause: Density and temperature, *Geophys. Res. Lett.*, *30*(16), 1869, doi:10.1029/2003GL017611.

Engwall, E., et al. (2009a), Survey of cold ionospheric outflows in the magnetotail, *Ann. Geophys.*, *27*, 3185–3201.

Engwall, E., et al. (2009b), Earth's ionospheric outflow dominated by hidden cold plasma, *Nat. Geosci.*, *2*, 24–27, doi:10.1038/ngeo387.

Escoubet, C. P., M. Fehringer, and M. Goldstein (2001), Introduction: The Cluster mission, *Ann. Geophys.*, *19*, 1197–1200.

Fear, R. C., et al. (2008), The azimuthal extent of three flux transfer events, *Ann. Geophys.*, *26*, 2353–2369.

Goldstein, J., B. R. Sandel, M. F. Thomsen, M. Spasojević, and P. H. Reiff (2004), Simultaneous remote sensing and in situ observations of plasmaspheric drainage plumes, *J. Geophys. Res.*, *109*, A03202, doi:10.1029/2003JA010281.

Khotyaintsev, Y., S. Buchert, K. Stasiewicz, A. Vaivads, S. Savin, V. O. Papitashvili, C. J. Farrugia, B. Popielawska, and Y.-K. Tung (2004), Transient reconnection in the cusp during strongly negative IMF B_y, *J. Geophys. Res.*, *109*, A04204, doi:10.1029/2003JA009908.

Khotyaintsev, Y. V., et al. (2006), Formation of inner structure of a reconnection separatrix region, *Phys. Rev. Lett.*, *97*(20), 205003, doi:10.1103/PhysRevLett.97.205003.

Laitinen, T. V., et al. (2010), Local influence of magnetosheath plasma beta fluctuations on magnetopause reconnection, *Ann. Geophys.*, *28*, 1053–1063, doi:10.5194/angeo-28-1053-2010.

Lindstedt, T., et al. (2009), Separatrix regions of magnetic reconnection at the magnetopause, *Ann. Geophys.*, *27*, 4039–4056.

McFadden, J. P., C. W. Carlson, D. Larson, J. Bonnell, F. S. Mozer, V. Angelopoulos, K.-H. Glassmeier, and U. Auster (2008), Structure of plasmaspheric plumes and their participation in magnetopause reconnection: First results from THEMIS, *Geophys. Res. Lett.*, *35*, L17S10, doi:10.1029/2008GL033677.

Mozer, F. S., S. D. Bale, and T. D. Phan (2002), Evidence of diffusion regions at a subsolar magnetopause crossing, *Phys. Rev. Lett.*, *89*(1), 015002, doi:10.1103/PhysRevLett.89.015002.

Owen, C. J., A. Marchaudon, M. W. Dunlop, A. N. Fazakerley, J.-M. Bosqued, J. P. Dewhurst, R. C. Fear, S. A. Fuselier, A. Balogh, and H. Rème (2008), Cluster observations of "crater" flux transfer events at the dayside high-latitude magnetopause, *J. Geophys. Res.*, *113*, A07S04, doi:10.1029/2007JA012701.

Paschmann, G. (2008), Recent in-situ observations of magnetic reconnection in near-Earth space, *Geophys. Res. Lett.*, *35*, L19109, doi:10.1029/2008GL035297.

Pedersen, A., et al. (2008), Electron density estimations derived from spacecraft potential measurements on Cluster in tenuous plasma regions, *J. Geophys. Res.*, *113*, A07S33, doi:10.1029/2007JA012636.

Retinò, A., et al. (2006), Structure of the separatrix region close to a magnetic reconnection X-line: Cluster observations, *Geophys. Res. Lett.*, *33*, L06101, doi:10.1029/2005GL024650.

Sauvaud, J.-A., et al. (2001), Intermittent thermal plasma acceleration linked to sporadic motions of the magnetopause, first cluster results, *Ann. Geophys.*, *19*, 1523–1532.

Tanaka, K. G., et al. (2008), Effects on magnetic reconnection of a density asymmetry across the current sheet, *Ann. Geophys.*, *26*, 2471–2483.

Vaivads, A., et al. (2004), Structure of the magnetic reconnection diffusion region from four-spacecraft observations, *Phys. Rev. Lett.*, *93*(10), 105001, doi:10.1103/PhysRevLett.93.105001.

Vaivads, A., et al. (2010), The Alfvén edge in asymmetric reconnection, *Ann. Geophys.*, *28*, 1327–1331, doi:10.5194/angeo-28-1327-2010.

M. André, Y. Khotyaintsev, T. Laitinen, and A. Vaivads, Swedish Institute of Space Physics, Box 537, SE-751 21 Uppsala, Sweden. (ma@irfu.se)

A. Fazakerley, Mullard Space Science Laboratory, Dorking RH5 6NT, UK.

H. Nilsson and G. Stenberg, Swedish Institute of Space Physics, Box 812, SE-981 28 Kiruna, Sweden.

J. G. Trotignon, Laboratoire de Physique et Chimie de l'Environnement et de l'Espace, Université d'Orléans, 3A, Av. de la Recherche Scientifique, F-45071 Orléans CEDEX 2, France.